



ARCHIVES
of
FOUNDRY ENGINEERING

DOI: 10.1515/afe-2016-0112

Published quarterly as the organ of the Foundry Commission of the Polish Academy of Sciences



ISSN (2299-2944)

Volume 16

Issue 4/2016

217 – 221

The Influence of Laser Surface Remelting on the Microstructure of EN AC-48000 Cast Alloy

J. Piątkowski^{a,*}, A. Grabowski^b, M. Czerepak^c^a Faculty of Materials Science and Metallurgy, Silesian University of Technology, Krasińskiego 8, 40-019 Katowice, Poland^b Poland Institute of Physics – CSE, Krzywoustego 2, 41-100 Gliwice, Poland^c Federal – Mogul Powertrain Gorzyce, Odlewników 52, 39-432 Gorzyce, Poland

* Corresponding author. E-mail address: jaroslaw.piatkowski@polsl.pl

Received 06.04.2016; accepted in revised form 01.06.2016

Abstract

Paper present a thermal analysis of laser heating and remelting of EN AC-48000 (EN AC-AlSi12CuNiMg) cast alloy used mainly for casting pistons of internal combustion engines. Laser optics were arranged such that the impingement spot size on the material was a circular with beam radius r_b changes from 7 to 1500 μm . The laser surface remelting was performed under argon flow. The resulting temperature distribution, cooling rate distribution, temperature gradients and the depth of remelting are related to the laser power density and scanning velocity. The formation of microstructure during solidification after laser surface remelting of tested alloy was explained. Laser treatment of alloy tests were perform by changing the three parameters: the power of the laser beam, radius and crystallization rate. The laser surface remelting needs the selection such selection of the parameters, which leads to a significant disintegration of the structure. This method is able to increase surface hardness, for example in layered castings used for pistons in automotive engines.

Keywords: Surface treatment, Al-Si alloys, Laser surface remelting, Rapid solidification

1. Introduction

A laser beam can be used in several ways to impart advantageous properties to the surface of aluminum alloys [1, 2]. The laser surface remelting is one of methods where remelting of thin surface layer is applied to improve metallic automotive components: reducing porosity, texturing or smoothing macro roughness, increase of hardness on large area or locally in the region inaccessible for other processing method (e.g. piston ring slots) [3]. The effectiveness of laser surface remelting processing depends on the thermal properties of the material as well as the laser process parameters – laser power density, spot size, and traverse velocity. The optical absorption is also the important parameter determining the energy of a laser beam transferring

radiation into workpiece during its laser surface remelting [4]. In a laser surface remelting high solidifications velocities and high temperature gradients are obtained. It is commonly known that the laser surface remelting create a fine, usually a cellular/dendritic structure sometimes with a higher solid solubility of alloying elements [5].

2. Scope and purpose of research

The purpose of this paper is to summarize some possible effects of the laser power density and time interactions on the solidification process that in turn has a impact on the resulting microstructure of AlSi12CuNiMg cast alloy after laser remelting.

To obtain the thermal aspects of the solidification process of the tested alloy, the cooling rates, temperature gradient at the solid – liquid interface and the solidification rate of the solid/liquid interface in melted zone were calculated from a heat flow model.

3. Materials and research method

The AlSi12CuNiMg cast alloy (in accordance with norm PN-EN 1706 EN AC-48000) was chosen for the tests. It was casted to sand moulds and casting dies and meant for i.e. castings of pistons of internal combustion engines, blocks, and cylinder bodies of compressors, pumps and brakes. The research material was the actual casting of the piston. In this investigation casted AlSi12CuNiMg alloy was studied. The tested alloy workpiece was 150 mm long, 50 mm wide, and 25 mm thick. The top surface of the workpieces were polished with DP-Spray, P, Struers-1 μm prior to laser surface melting in order to produce a smooth surface with roughness parameter $Ra = 0,93 \mu\text{m}$. The workpieces were mounted on a numerical controlled X-Y table and irradiated by a CW disc laser emitting electromagnetic radiation with the wavelength of 1,03 μm . and the Gaussian power densities distribution. Laser optics were arranged such that the impingement spot size on the material was a circular with beam radius r_b changes from 7÷1500 μm . The laser surface melting was performed under argon flow. The optical absorptions $A(=I-R)$ of the AlSi12CuNiMg alloy workpieces was estimated by reflectance measurements. The total optical reflectance (R) was measured by use of an integrating sphere (ISP-REF, Ocean Optics Inc.) equipped with a spectrophotometer HR4000 CG-UV-NIR [6].

The effect of power density and time interactions on the surfaces laser melting process of AlSi12CuNiMg alloy, was investigated in the experimental arrangement showed at Figure 1a. The following coordinate system fixed in the material was used: the laser beam was parallel to the “z” axis and the laser beam moves in the “x” direction with the vector of scanning speed v_b . The laser beam used was moved with constant relative scanning speed to the surface of investigated alloy. The traces formed on the plates were resulting from laser treatment. The applied laser treatment was characterized by appropriate power densities and time interactions that were determined from the relation:

$$t_L = \frac{2 \cdot r_b}{v_b} \quad (1)$$

In the experiments the scanning speed of the beam was changed in the range of (0,5÷1) $\text{m} \cdot \text{min}^{-1}$. The laser power density for the circular laser beam with radius r_b that is used in the experiments is calculated from the relation [6]:

$$I_0 = \frac{P}{\pi \cdot r_b^2} \quad (2)$$

where P is the power of the laser beam.

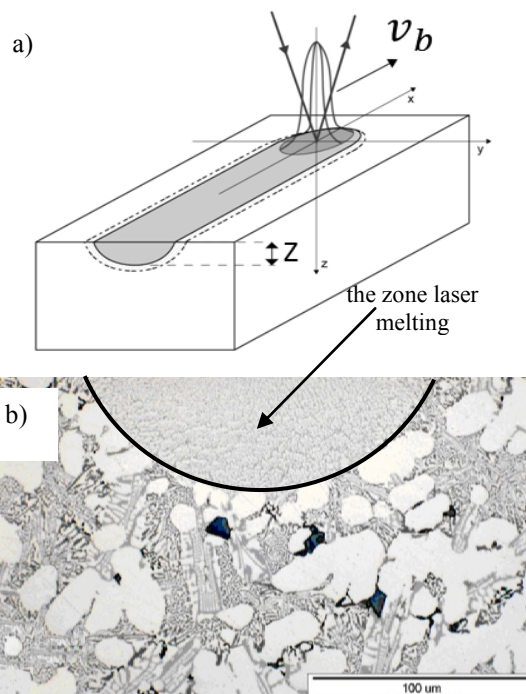


Fig. 1. a) Schematic illustrating laser surface melting by a scanning laser beam moving in the x-direction at a constant velocity v_b ; b) microstructures of cross section of laser remelted zone in alloy with operating conditions:

$$P = 50 \text{ W}; v_b = 1 \text{ m} \cdot \text{min}^{-1}; r_b = 7 \mu\text{m}$$

In each experiment the power density of the laser beam was changed by adjustment of the power and radius of the laser beam. Selection of the operating parameters: v_b ; P ; r_b is related to expected AlSi12CuNiMg solidification rate after laser remelting as it is presented in the remaining part of this study. The treated surfaces of tested alloy plates were sectioned at 90° to the direction of the beam travel. Next the standard metallographic preparation was made. Metallographic changes induced by laser treatment were investigated by optical microscope Olympus GX71. Fig. 1b shows the cross sectioned of the AlSi12CuNiMg cast alloy plate after laser melting with the $P = 50 \text{ W}$; $v_b = 1 \text{ m} \cdot \text{min}^{-1}$; $r_b = 7 \mu\text{m}$.

The theoretical part of this study is based on well-tested heat flow model proposed by Asby and Esterling [7]. The model is used to analyze how changes in the laser processing parameters $I_0 A$; v_b and r_b can impact the melt depth, and solidification rate during laser surface melting of tested alloy. The model uses a Cartesian coordinate system presented in Figure 1a, the temperature $T(z, t)$ distribution immediately below the centre of the beam ($y = 0$) is given by [8]:

$$T(z, t) = T_{\perp 0} + \frac{I_{\perp 0} \cdot A}{2r_{\perp} b(-2) \cdot v_{\perp} b \cdot K \sqrt{t(t+t_{\perp 0})}} \cdot \exp\left[-\frac{(z+z_o)^2}{4\kappa t}\right] \quad (3)$$

where:

$$z_o = \left[\frac{\pi \kappa r_b}{2e v_b}\right]^{\frac{1}{2}} T(z, t) \quad (4)$$

is the temperature as a function of depth z and time t ,
 K – thermal conductivity,
 k – thermal diffusivity.

The model assumes that the thermophysical properties are independent of temperature. In this calculations values of thermo physical parameters for the solid alloys were used, averaged over the considered temperature range.

4. The results of investigations

Chemical composition of AlSi12CuNiMg alloy is presented in Table 1.

Table 1.

Chemical composition of the AlSi12CuNiMg cast alloy

Alloy	Si	Cu	Mg	Ni	Ti	Mn	Fe	Al
ENAC 48000	11,43	1,28	0,92	1,24	0,03	0,11	0,41	rest

The typical quality defects are [9, 10]:

- vesicles in rings and on the connection line with the piston,
- metallic and non-metallic inclusions by the insert,
- no adherence of the „alphin” ring (insert),
- improper ring diameter,
- cavities porosity on the connection with the piston (Fig. 2).



Fig. 2. Shrinkage cavity on the connection place of ring with the piston

The microstructures of the tested cast alloy after laser remelting for three different operating conditions are shown at:

- $v_b = 1\text{ m}\cdot\text{min}^{-1}$; $P = 50\text{ W}$; $r_b = 7\ \mu\text{m}$ - Figure 1b
- $v_b = 1\text{ m}\cdot\text{min}^{-1}$; $P = 600\text{ W}$; $r_b = 100\ \mu\text{m}$ - Figure 3a

$v_b = 1\text{ m}\cdot\text{min}^{-1}$; $P = 2000\text{ W}$; $r_b = 1500\ \mu\text{m}$ - Figure 3b

Microanalysis of the three aforementioned structures shows that the laser treatment causes the primary solid solution $\alpha(\text{Al})$ and $\alpha(\text{Al}) - \beta(\text{Si})$ eutectic to be finer by comparison to the remelted zone of as-cast state.

As a result of the rapid solidification of the laser-melted zone, finer grains were formed near the surface ($z = 0$), and columnar crystals were produced along the heat-flow direction near to the base of the treated material. To correlate the microstructure with the employed laser operating parameters, an attempt has been made to predict the thermal profile and related thermal history (heating/cooling rate, thermal gradient) resulting from the present laser treatment through numerical solution of the heat flow equation (Fig. 1). In this solution the average values of tested cast alloy over the temperature range of thermal conductivity $K = 115,7\text{ W}\cdot\text{K}\cdot\text{m}^{-1}$ and thermal diffusivity $k = 42\cdot 10^{-6}\text{ m}^2\cdot\text{s}^{-1}$ – were used. The value of absorptance $A = 0,11$ measured for cast alloy surface in room temperature was used.

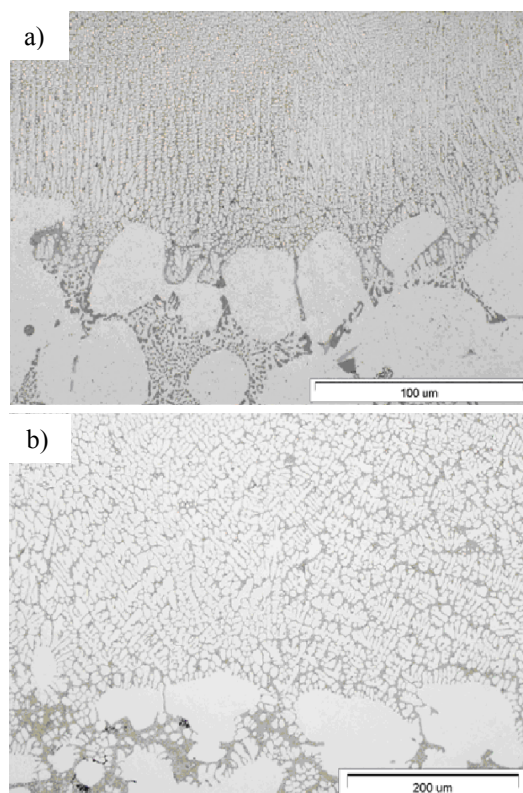


Fig. 3. Microstructures of cross section of laser remelted layer in AlSi12CuNiMg cast alloy with operating conditions:

- a) $v_b = 1\text{ m}\cdot\text{min}^{-1}$; $P = 600\text{ W}$; $r_b = 100\ \mu\text{m}$;
- b) $v_b = 1\text{ m}\cdot\text{min}^{-1}$; $P = 2000\text{ W}$; $r_b = 1500\ \mu\text{m}$

Figure 4 shows three calculated temperature cycles in laser surface melting with laser parameters described at Figure 3b. The remelting process includes heating and melting of AlSi12CuNiMg fast cooling and solidification. The maximum temperature at the surface ($z = 1\ \mu\text{m}$) being higher than melting point of tested alloy

(888 K) and silicon melting (1685 K) but should be lower than vaporization temperature of aluminum (2793 K).

The middle curve shows the temperature history at depths of the AlSi12CuNiMg alloy $z = 200\mu\text{m}$. The time at which the temperature at this depth reaches the highest value of 1273 K is 2,1 ms. Next the treated material begins self-cooling and the temperature falls till it reaches the melt temperature and solidifies at time 6,75 ms. The locus of depths “ z ” at times when the temperature equals melt temperature $T_{m(\text{AlSi12})} = 888\text{ K}$, defines the position of the solid - liquid interface as a function of time during solidification [8]. Temperature versus time at various depths “ z ” for varied $(0,2\div 3,6)\cdot 10^{10}\text{ W}\cdot\text{m}^{-2}$ and $v_b=(0,5\div 1)\text{ m}\cdot\text{min}^{-1}$ are computed from Fig.1 and the procedure for determining the time solidification has been applied. The slope of the solid-liquid interface position versus time is proportional to the solidification rate. The computed solid-liquid interface velocity during solidification of an alloy along the “ z ” for various combinations of laser parameters v_b ; P ; r_b values is shown in Figure 5.

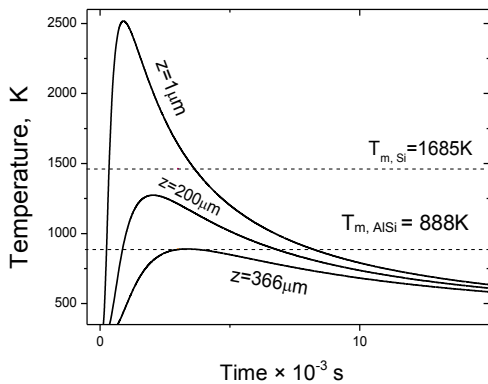


Fig. 4. Calculated temperature cycles on the AlSi12CuNiMg at selected melt depths versus time

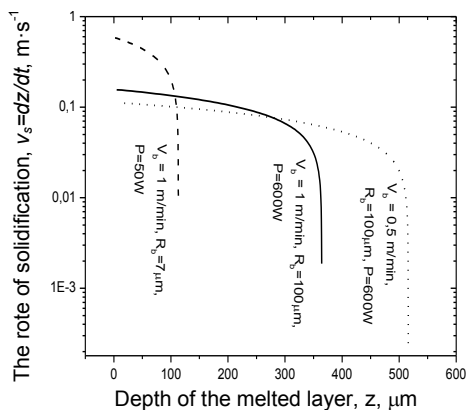


Fig. 5. Laser surface remelting of tested alloy. Calculated results for three different laser parameter v_b ; P ; r_b showing the evolution of solidification rate v_s as a function of depth

The position of the solid-liquid interface as a function of time computed from (1) could also determine the cooling rate:

$$T = \frac{dT}{dt} \quad (5)$$

and the temperature gradient

$$G = \frac{dT}{dz} \quad (6)$$

The variation of cooling rate (T) and gradient (G) at the melt interface of AlSi12CuNiMg with the melt depth computed from (1) is shown in Figure 6.

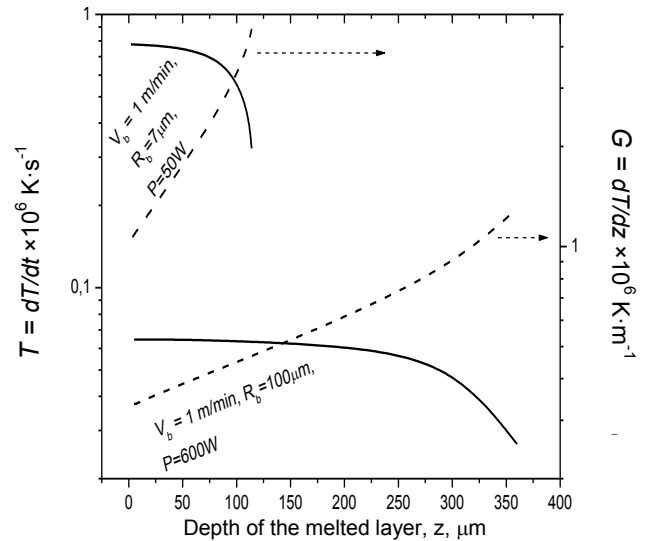


Fig. 6. Laser surface remelting of AlSi12CuNiMg. Calculated results for two different laser parameter v_b and P showing the evolution of cooling rate T (5) and temperature gradient G (6) as a function of depth

As can be shown the gradient has a maximum value at the start of solidification (the bottom position of the melted zone) and approaches zero as the surface of AlSi12CuNiMg solidifies. The values of gradient is a function of l_0 and time interactions t_L the highest values of $G=7,8\cdot 10^6\text{ K}\cdot\text{m}^{-1}$ was obtained for the next laser parameters: $v_b = 1\text{ m}\cdot\text{min}^{-1}$; $P = 50\text{ W}$ and $r_b = 7\mu\text{m}$.

Presented at Figure 5 dependences of solidification rate at the melt interface as a function of depth for three different sets of laser parameters shows individual influence of v_b ; P and r_b . The increase of the product $P\cdot v_b^{-1}$ values causes the increase in melt depth.

The decreases of radius r_b at constant value of P leads to the increase of laser power density l_0 but small radius in combination with large v_b (small time interaction t_L give the highest values of cooling rate:

$$T = \frac{dT}{dt} = 7,8\cdot 10^6\text{ K}\cdot\text{s}^{-1} \quad (7)$$

during laser surface melting of AlSi12CuNiMg cast alloy, as it is presented in the Figure 6.

Figures 5 and 6 show the evolution of changes solidification rate v_s and temperature gradient G as a function of depth. As solidification begins, the gradient is large, while the solidification

rate is almost zero, thus the ratio $\frac{G}{v_s}$ have maximum values. As

solidification approaches the surface ($Z \approx 0 \mu\text{m}$) the gradient which is continuously decreasing tends to zero while the v_s which is continuously increasing tends to maximum value.

5. Summary

In this study the influence of the following laser parameters: v_b ; P and r_b used during laser surface remelting process of EN AC-48000 (AlSi12CuNiMg) cast alloy has been investigated. Figure 5 shows that the solidification rate v_s at employed laser parameters changes in the range $(0,008 \div 0,6) \text{m} \cdot \text{s}^{-1}$. The highest value of v_s obtained in this study is lower in comparison to Mullins and Sekerka's theory of stability solidification planar front growth. According to the Mullins and Sekerka's theory the upper value for AlSi12CuNiMg (EN AC-48000) cast alloy reaches the value of approximately $35 \text{m} \cdot \text{s}^{-1}$ [11].

It can be clearly observed in the microstructures presented in the Figures 1b and 3a, that the resulting laser remelted zone, exhibits very refined microstructure. The refined dendrites grow in correlation to the temperature gradient. The dendrites tend to be perpendicular to the actual position of the solid – liquid interface, leading to specific orientation. At the top part of the remelting zone ($Z \approx 0 \mu\text{m}$), where v_s is the highest, the dendrites gradually lose their secondary branches and become more cellular in their character. Such changes are clearly in accordance with the calculated solidification rate gradient (Figures 5 and 6), since $G \cdot v_s$ give rise to a finer structure.

References

- [1] Watkins, K., McMahon, M. & Steen, W. (1997). Microstructure and corrosion properties of laser surface processed aluminum alloys. *Materials Science and Engineering*. 231(1-2), 55-61.
- [2] Tański, T., Makiela, W., Janicki, D., Tomiczek, B. & Król, M. (2016). Properties of the aluminum alloy EN AC-51100 after laser surface treatment. *Archives of Metallurgy and Materials*. 61(1), 199-204.
- [3] Kusiński, J., Kaç, S., Kopia, A., Radziszewska, A., and other. (2012). Laser modification of the materials surface layer – a review paper. *Bulletin of the Polish Academy of Sciences - Technical Sciences*. 60(4), 711-728.
- [4] Grabowski, A. (2013). *The interaction of the laser beam composites silumin – SiC particles*. Gliwice: Silesian University of Technology, 30-40. (in Polish).
- [5] Jones, H. (1984). The status of rapid solidification of alloys in research and applications. *Journal of Material Science*. 19(4), 1043-1076.
- [6] Nowak, M., Bober, Ł., Borkowski, B., Kępińska, M., Szperlich, P., Stróż, D. & Sozańska, M. (2013). Quantum efficiency coefficient for photogeneration of carriers in SbSI nanowires. *Optical Materials*. 35, 2208-2216.
- [7] Ashby, M. & Easterling, K. (1984). The transformation hardening of steel surfaces by laser beams - I. Hypoeutectoid steels. *Acta Metallurgica*. 32(11), 1935-1948.
- [8] Bass, M. (1983). *Laser materials processing*. Elsevier Science Publishing Company Inc., 238-260.
- [9] Piątkowski, J. & Kamiński, P. (2015). Chosen Aspects of Quality Defects of “Alphin” Inserts in Combustions Pistons. *Archives of Foundry Engineering*. 15(4), 61-65.
- [10] Piątkowski, J. (2015). AlSi17Cu5Mg alloy as future material for casting of pistons for internal combustion engines. *Metalurgija*. 54(3), 511-514.
- [11] Mullins, W. & Sekerka, R. (1964). Stability of planar interface during solidification of dilute binary alloy. *Journal of Applied Physics*. 35, 444-451.